GEOFLUIDS

Geofluids (2011) **11**, 328–340 doi: 10.1111/j.1468-8123.2011.00343.x

Thermodynamic modeling of petroleum inclusions: the prediction of the saturation pressure of crude oils

H. PING[1,2], R. THIÉRY[3,4,5] AND H. CHEN[1,2]

[1]*Department of Petroleum Geology, Faculty of Earth Resources, China University of Geosciences, Wuhan, China;* [2]*Key Laboratory of Tectonics and Petroleum Resources (China University of Geosciences), Ministry of Education, Wuhan, China;* [3]*Clermont Université, Université Blaise Pascal, Laboratoire Magmas et Volcans, Clermont-Ferrand, France;* [4]*CNRS, UMR 6524, LMV, Clermont-Ferrand, France;* [5]*IRD, R 163, Clermont-Ferrand, France*

ABSTRACT

Microthermometry and volumetric analysis are now widely used techniques in petroleum geology, which allow the reconstitution of the composition and *P-T* trapping conditions of petroleum inclusions. However, these methods require efficient thermodynamic modeling tools of the PVT properties, coupled with compositional models for petroleum. Two methods presently available are reviewed here. The first one, called the α–β method, uses a compositional model describing the full spectrum (C_1–C_{500}) of natural hydrocarbons with two adjustable parameters α and β. The second technique is based on a so-called fluid model, i.e., *a priori* knowledge of the composition and the physical properties of the C_{7+} cut of the trapped petroleum. Up to now, no critical appraisal has been undertaken for these two methods. From an extensive compilation of literature data (201 points), we here show that both techniques are able to describe the composition of crude oils and to predict satisfactorily their saturation pressures. However, the predictive capabilities of fluid models are highly dependent on the correlations used for describing heavy cuts, and we indicate those which give the best results. Finally, we emphasize the key control of the bulk methane mole fraction (x_1) on the saturation pressure: this result allows us to build simplified versions of α–β and fluid models, applicable to the majority of crude oils, and whose formulation depends advantageously on x_1 only.

Key words: petroleum inclusion, saturation pressure, thermodynamic

Received 27 January 2011; accepted 22 June 2011

Corresponding author: Hongwei Ping, Department of Petroleum Geology, Faculty of Resources, China University of Geosciences, Lumo road No.388, Hongshan District, Wuhan 430074, Hubei Province, China.
Email: howping@yahoo.cn. Tel: +86 27 67848512. Fax: +86 27 67883051.

Geofluids (2011) **11**, 328–340

INTRODUCTION

There is an increasing interest for the study of petroleum inclusions, in particular, for the reconstruction of the composition and the *P-T* path evolution of migrating petroleum in sedimentary basins (Munz 2001). However, the procedure for interpreting the analytical data is not simple and must follow a schematic flow (steps 1–3), as illustrated in Fig. 1A. The first step relies on simple analytical techniques, such as (i) microthermometry (Roedder 1984; Goldstein & Reynolds 1994) to measure the homogenization temperatures T_h and (ii) volumetric determinations (Pironon *et al.* 1998) of the degrees of bubble filling (F_v) at various temperatures. These data provide some constraints about the bulk composition of petroleum fluid inclusions. The second step aims to estimate the *in situ* homogenization pressure P_h by appropriate thermodynamic modeling. This part is the most sensitive, as the composition of the trapped petroleum cannot be constrained fully by microthermometry and volumetric analysis. Thus, some assumptions about the petroleum composition have to be stated, and for this reason, it is necessary to use a so-called compositional model (De Hemptinne & Béhar 2006) for natural hydrocarbon mixtures (Aplin *et al.* 1999; Thiéry *et al.* 2002). By this method, the problem of composition indetermination by an iterative process can be alleviated, where the hypothesized oil composition is tuned to a perfect matching of modeled T_h and F_v with their observed counterparts. The third and last step is the calculation of the trapping $P_t - T_t$

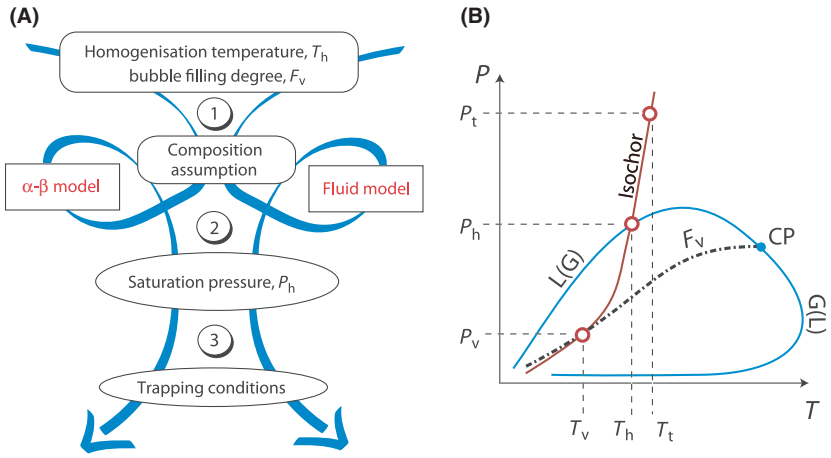

Fig. 1. (A) Schematic view of the different steps for interpreting microthermometric data. (B) Typical *P-T* phase diagram of a petroleum, illustrating the different elements required for the analysis of microthermometric and volumetric data. The liquid–gas immiscibility loop is delimited by the bubble point L (G) curve and the dew point G(L) curve, joining at the critical point (CP). The *P-T* path of the inclusion is described by an isochore, whose three points are of interest: the (P_t, T_t) trapping point, the (P_h, T_h) homogenization point, and the (P_v, T_v) point, at which the degree of bubble filling, F_v, is measured. The dashed–dotted curve is one isocurve of constant F_v.

conditions (see Munz *et al.* 1999; Chen *et al.* 2003 for application examples of this analysis technique for petroleum inclusions). Figure 1B illustrates a typical *P-T* phase diagram of an example petroleum, giving the basics for the interpretation of microthermometric and volumetric data.

Two different approaches can be identified for compositional models used for analyzing petroleum inclusions. The first one, called here the α–β model, involves two adjustable parameters, α and β, to approximate the full compositional spectrum (C_1–C_{500}) of natural oils (Montel 1993; Thiéry *et al.* 2002), whereas the second one (the so-called fluid model) uses postulated compositional data (Macleod *et al.* 1996; VTFlinc 1997; Aplin *et al.* 1999; Munz *et al.* 1999), mainly, in the form of mole percentages for C_1, C_2, C_3, C_4, C_5, C_6, and C_{7+} and physical properties, MW_{7+} and SG_{7+}, respectively, the molar weight and specific gravity of the C_{7+} cut. Next, the compositional model must be coupled with a thermodynamic model to predict the physico-chemical properties of petroleum. This thermodynamic modeling includes the use of (i) correlations for describing the physical parameters of the different petroleum cuts and (ii) an equation of state for PVT and phase equilibria calculations. As it will be shown in this study, the integrated use of compositional and thermodynamic models requires a calibration (or at least, testing and validation) against experimental data.

The determination of trapping conditions (step 3 in Fig. 1) is directly dependent on the accuracy of the homogenization pressure P_h calculated previously, and this is the main point addressed by this article: how to be confident about the precision of thermodynamic/compositional models used for predicting the saturation pressure of crude oils? Indeed, to our knowledge, nothing has been yet reported in the literature about the prediction of such thermodynamic modeling for petroleum inclusions, mainly because of the lack of published data (Thiéry *et al.* 2002). However, in the last decade, numerous PVT studies have been made publicly available [e.g., see (Elsharkawy 2003) and references therein], which may shed a new light on this problem. The article is structured thus:

(1) The first part revisits the α–β model, and from the data compilation cited earlier, we have obtained a collection of α–β points representative of petroleum. After an error analysis of this compositional model, we show that the α–β model is able to represent the large diversity of petroleum composition and homogenization pressure P_h by means of two parameters (α and β) only;

(2) Subsequently, however, we show that microthermometric and volumetric measurements are not sufficient by themselves to determine unambiguously the α and β parameters of trapped petroleum in fluid inclusions. As a consequence, we propose a simplification of the α–β model toward a compositional model depending only upon one parameter (the β model);

(3) The validity of this model simplification is next discussed, and we demonstrate that one important point to address in the future, to get more precise P_h pressures, is to quantify the bulk methane content;

(4) Finally, we go back to fluid models and test several correlations for calculating the thermodynamic properties of the C_{7+} cut to obtain accurate saturation pressures.

The α–β model

Basics

During and after their migration into reservoirs, petroleum can be modified by numerous processes, such as boiling, condensation, mixing, biodegradation, oxidation, gas leaching, water washing, or secondary cracking. Despite all of these processes, the composition of oils can be represented, to a first approximation, by the following recurrent relation (Montel 1993):

$$x_{n+1} = \alpha \cdot \left(1 - \frac{\beta}{n+1}\right) \cdot x_n, \quad (1)$$

where x_n and x_{n+1} are the mole fractions of cuts with n and $n + 1$ atoms of carbon. In Eq. 1, α and β are two adjustable parameters, which are obtained by regression on compositional data. The α parameter describes the geometric distribution of nonvolatile, heavy hydrocarbons (with $n > 10$) as a function of n, as this has been well evidenced for n-alkanes in petroleum crudes (Kissin 1987; Munz *et al.* 1999) with typical α values ranging between 0.60 and 0.91. The β parameter is most influential for the abundance of volatiles hydrocarbons (C_1–C_6). A positive value of β indicates the enrichment of the volatile part, whereas negative β values signify a strong depletion of the petroleum in its volatile fraction. Thus, in practice, β values range between −0.2 and 1. This study uses a more elaborate version of Eq. 1 (Montel, private communication; Thiéry *et al.* 2002), which provides a more realistic representation of petroleum compositions. This modified alpha–beta model is the same as that used in numerous publications (Teinturier *et al.* 2002; Thiéry *et al.* 2002; González-Partida *et al.* 2003; Guillaume *et al.* 2003; Bourdet *et al.* 2008, 2010), illustrating the applicability of the alpha–beta model to fluid inclusion studies. While the detailed equations have not been published, free calculation software is available (see Acknowledgements section), which allows the recalculation of theoretical composition spectra and phase diagrams from specified alpha and beta values. Figure 2 shows the (α–β) space, where the different petroleum categories, as defined by (McCain Jr. WD 1994), have been mapped. This diagram is also useful to plot the different α–β values satisfying a given set of T_h and F_v, which can be measured individually on one petroleum inclusion (Thiéry *et al.* 2002). Indeed, because of the problem of composition indetermination, there is no unique solution, and the full set of solutions is represented by an α–β curve (Thiéry *et al.* 2000, 2002; Pironon 2004); for example, for an inclusion featured by T_h = 54.41°C and F_v = 3% measured at 20°C, the α–β solutions are given by the dotted curve with vertical bar [β(α)] drawn in Figure 2. For the sake of illustration, we have chosen three representative points, whose calculated characteristics are given in Table 1. Corresponding α–β points are plotted in Figure 2.

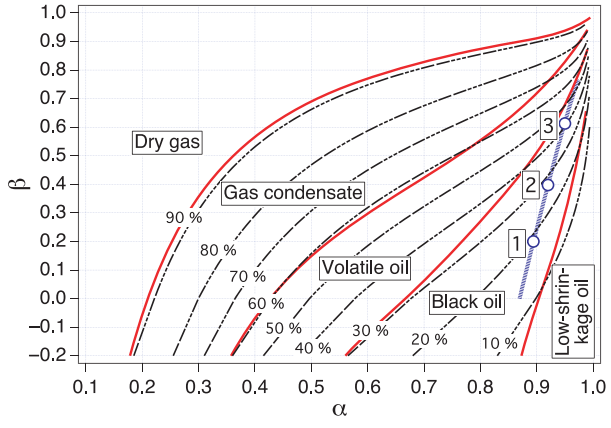

Fig. 2. The α–β space. The full lines delimit the fields of different petroleum types defined by the classification of McCain Jr. WD (1994). The numbered and long dashed curves are isocurves of C_1 mole percent. The dotted line with vertical bar is an example of an α(β) curve calculated for a petroleum inclusion (see text for details). The three numbers 1, 2, and 3 refer to α–β fluid detailed in Table 1.

As it can be noted, these three compositions calculated by the α–β model yield discrepant saturation pressures. This example illustrates the difficulty in making barometric estimations in petroleum inclusions on the basis of only microthermometric and volumetric measurements. Additional information on the oil composition is thus invaluable (Thiéry *et al.* 2002). This can be obtained by gas chromatography of fluid aliquots released by sample crushing (Munz *et al.* 1999; George *et al.* 2007). However, the applicability of this technique can be limited by sample pollution or mixing of several fluid generations. Fourier-transform infrared microspectroscopy (FT-IR) can also provide an useful indication of the bulk methane content (Pironon *et al.* 2001), as this constrains the position of the α–β point in the α–β space (Figure 2 and Table 1). However, the technique is not applicable for inclusions smaller than 10 μm.

Model testing

To test the adequacy of the α–β model to describe the composition and saturation pressure of crude oils, we have used mainly the data compilation provided by Elsharkawy 2003 (126 points) plus 75 points from other recent studies. The data sources are given in Table 2 and comprise 201 bubble point pressures data. Figure 3 illustrates the dependence of the saturation pressure P_h as a function of the C_1 mole percent. Saturation pressure ranges between 20 and 475 bar. The saturation temperatures T_h are between 20 and 160°C, thus covering the typical range of homogenization temperatures of petroleum inclusions.

Table 1 Characteristics of three possible α–β solutions for a petroleum inclusion featuring a T_h = 54.4°C and a F_v = 3% at 20°C.

Solution	α	β	P_h (bar)	x_1 (mole %)	x_{7+} (mole %)
1	0.894	0.200	55	18.6	55.5
2	0.920	0.398	89	27.1	48.3
3	0.950	0.613	186	41.7	38.1

Table 2 References of experimental data from the literature (*P-T* composition conditions of petroleum saturations).

References	Number of points
Agarwal *et al.* (1990)	1
Ahmed (1989)	2
Al-Meshari (2004)	21
Avaullée *et al.* (1997)	4
Coats & Smart (1986)	7
Danesh *et al.* (1992)	8
Drohm *et al.* (1988)	1
Elsharkawy (2003)	58
Hoffman *et al.* (1953)	2
Hong (1982)	2
Jacopy & Berry (1958)	1
Jaubert *et al.* (1995)	10
Jaubert *et al.* (2002)	11
Jhaveri & Youngren (1988)	2
Li *et al.* (1985)	1
McCain Jr. WD (1990)	1
Moharam (1995)	7
Neau *et al.* (1993)	14
Pedersen *et al.* (1988a,b)	9
Riemens *et al.* (1988)	1
Rosenegger & Wu (1999)	22
Vogel & Yarborough (1980)	1
Wang & Gmehling (1999)	10
Williams *et al.* (1980)	1
Yang *et al.* (1997)	4

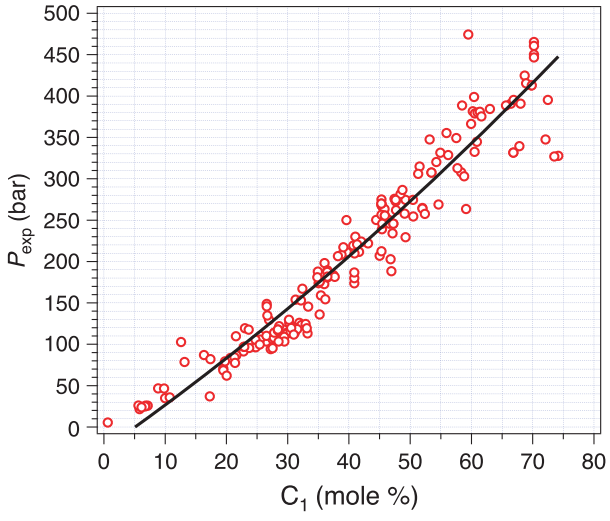

Fig. 3. Experimental bubble point pressures as a function of the C_1 mole percent. The solid line is a polynomial curve, which has been calculated by linear regression of the experimental data.

Our intention is to find the best-fitting α and β values to represent the composition and homogenization pressure P_h for each fluid of the data bank. For this purpose, the following objective functions, F_1 and F_2, have been minimized simultaneously by using a standard optimization algorithm:

$$F_1(\alpha,\beta) = (x_{1,\mathrm{calc}} - x_{1,\mathrm{exp}})^2 + (x_{2,\mathrm{calc}} - x_{2,\mathrm{exp}})^2 + (x_{3,\mathrm{calc}} - x_{3,\mathrm{exp}})^2 + (x_{4,\mathrm{calc}} - x_{4,\mathrm{exp}})^2 + (x_{5,\mathrm{calc}} - x_{5,\mathrm{exp}})^2 + (x_{6,\mathrm{calc}} - x_{6,\mathrm{exp}})^2 + (x_{7,\mathrm{calc}} - x_{7,\mathrm{exp}})^2 \quad (2)$$

and

$$F_2(\alpha,\beta) = (P_{h,\mathrm{calc}} - P_{h,\mathrm{exp}})^2 \quad (3)$$

The resulting α–β points are given in the α–β space in Fig. 4: α values were found to lie between 0.78 and 0.97, whereas β parameters range between −0.26 and 0.76. The α–β points form a rather dispersed set of points with no obvious trend.

To check the accuracy of the model, we compare experimental and calculated values of pressure and composition. To measure the composition discrepancies, we consider the absolute deviation, Δx, and the relative mean square error, δx, of the mole fractions xi of different cuts (C_1, C_2, C_3, C_4, C_5, C_6, C_{7+}), defined, respectively, by:

$$\Delta x = \sum_{i=1}^{7+} \left| \frac{x_{i,\mathrm{calc}} - x_{i,\mathrm{exp}}}{x_{i,\mathrm{exp}}} \right| \quad (4)$$

$$\sigma x = \sqrt{\frac{1}{7}\sum_{i=1}^{7+} (x_{i,\mathrm{calc}} - x_{i,\mathrm{exp}})^2} \quad (5)$$

Next, deviations between experimental and calculated values are quantified by means of classical statistical parameters:

ARD (P), the average relative deviation, defined by:

$$\mathrm{ARD}(P) = \frac{1}{N}\sum_{i=1}^{N} \frac{P_{\mathrm{calc}} - P_{\mathrm{exp}}}{P_{\mathrm{exp}}} \quad (6)$$

AAD (P), the average absolute deviation, defined by:

$$\mathrm{AAD}(P) = \frac{1}{N}\sum_{i=1}^{N} \left| \frac{P_{\mathrm{calc}} - P_{\mathrm{exp}}}{P_{\mathrm{exp}}} \right| \quad (7)$$

or RMS (P), the relative mean square error, defined by:

$$\mathrm{RMS}(P) = \sqrt{\frac{1}{N}\sum_{i=1}^{N} \left(\frac{P_{\mathrm{calc}} - P_{\mathrm{exp}}}{P_{\mathrm{exp}}}\right)^2} \quad (8)$$

where N is the number of data points and P is either the methane mole fraction x_1 or the pressure P.

A summary of comparison results is given in Table 3. A close agreement between the model and data is obtained. The AAD (P) on the saturation pressure is only 0.8%. The mean of absolute deviations, Δx, for the composition of different cuts are above 23%. This large value is because of the rather high variability of C_2, …, C_6 mole percents in petroleum, but this does not impair the quality of the model, as the AAD (x_1) for methane composition is below 10%. Thus, the α–β model is highly appropriate for representing the composition spectrum and the saturation pressure of crude oils under the P-T conditions of reservoirs.

Model simplification

While an inspection of Fig. 4 shows no evident correlation between α and β, a strong correlation between these two parameters was revealed by our fitting program (with a correlation coefficient above 0.98). Thus, the fit is ill-conditioned and it is worth reducing the number of fitting parameters. However, the variation range of α (around 0.2) is smaller than the variation interval of β (about 1.1). Thus, we choose to retain a mean value of 0.92 for alpha and perform a new fit by using only one adjustable parameter, i.e., β. For this reason, this model will be called the β model.

Resulting α–β points are plotted in Fig. 4 and are aligned vertically in this α–β space. Mathematically, this operation corresponds to the projection of α–β points, previously calculated using the α–β model, onto the line $\alpha = 0.92$ by following the isocurves of constant C_1 mole percent (Fig. 4).

The accuracy of the model can be checked as above in Table 3. There is a slight degradation of the model in representing the composition, but the simplified model remains acceptable. Moreover, the β model is found to be slightly more accurate for the saturation pressure [AAD (P) of 0.23% instead of 0.8%]. Thus, from this point of view, the β model can be considered as good as the α–β model.

Table 3 Summary of fitting results of α–β models with respect to experimental data.

Parameters	Unit	α–β model	β model
Mean (Δx)	%	23.8	30.1
Mean (σ_x)	mole %	1.8	3.1
ARD (x_1)	%	9.8	7.1
AAD (x_1)	%	9.3	9.9
RMS (x_1)	mole %	3.6	4.9
ARD (P)	%	−0.4	0.02
AAD (P)	%	0.8	0.23

Mean (Δx), mean absolute deviation between experimental and calculated composition; Mean (σ_x), mean relative mean square error between experimental and calculated composition; ARD, average relative deviation; RMS, relative mean square error; AAD, average absolute deviation.

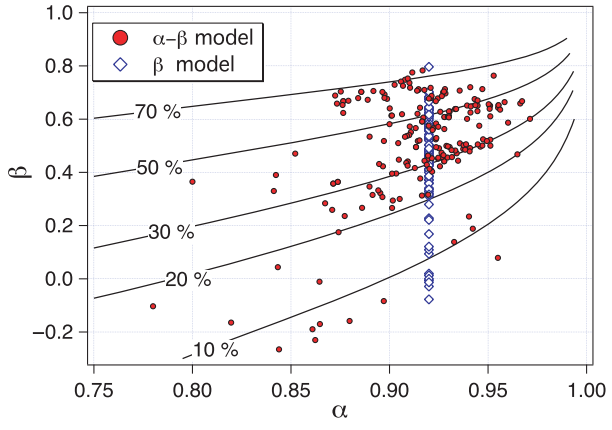

Fig. 4. Fitted α–β points from literature data (composition and saturation pressure) for crude oils. The filled circles have been calculated from data regression with the initial α–β model, whereas the empty diamonds are obtained using the simplified β model. The solid lines are isocurves of constant C_1 composition (the percentages refer to the bulk mole percents of methane).

Application to petroleum inclusions

As the β model describes satisfactorily the composition and saturation pressures of crude oils, it is tempting to use it instead of the more general α–β model. There are at least two motivations for this choice:

(1) the narrower α–β domain defined by $0.85 \le \alpha \le 0.95$ and $0.35 \le \beta \le 0.7$ is the field that is relevant (Thiéry *et al.* 2002) to the majority of crude oils. This is also the region, where the β model approximates at best the α–β model.

(2) this approach reduces the number of independent parameters to only one (i.e., β).

Moreover, it has been found that β can be easily correlated as a function of experimental mole fraction (x_1) of methane. This correlation is illustrated in Fig. 5 and is given by:

$$\beta = 0.77474 - 0.97186 \exp(-3.8104 x_1) \qquad (9)$$

As stated earlier, the methane composition can be measured by FT-IR spectroscopy (Pironon *et al.* 2001). Thus, this technique, coupled with this thermodynamic model, permits the unambiguous estimation of the *in situ* homogenization pressure P_h of oil-bearing fluid inclusions. Following a suggestion by Bourdet *et al.* (2008), this could permit the deciphering of the natural relations that seem to exist between observed T_h, F_v, or x_1 of petroleum inclusions.

The accuracy of the beta model coupled with Eq. 9 has been tested below. Calculated pressures are compared with experimental values, and a close agreement is obtained (Table 4, Fig. 6). This β model has also been compared with the relationship, given in Elsharkawy (2003) and

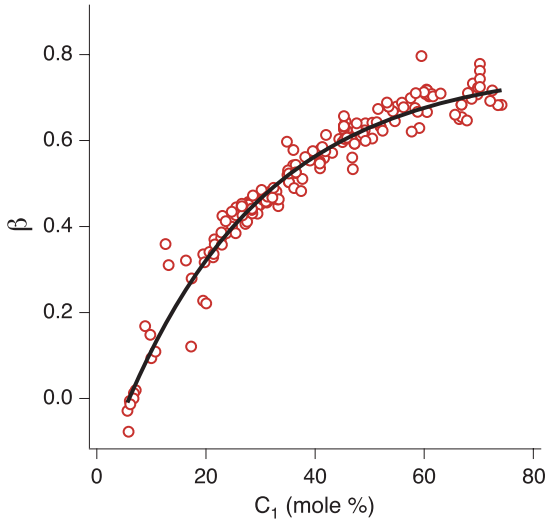

Fig. 5. Regression curve of β parameters (obtained from the β model) as a function of experimental C_1 mole %.

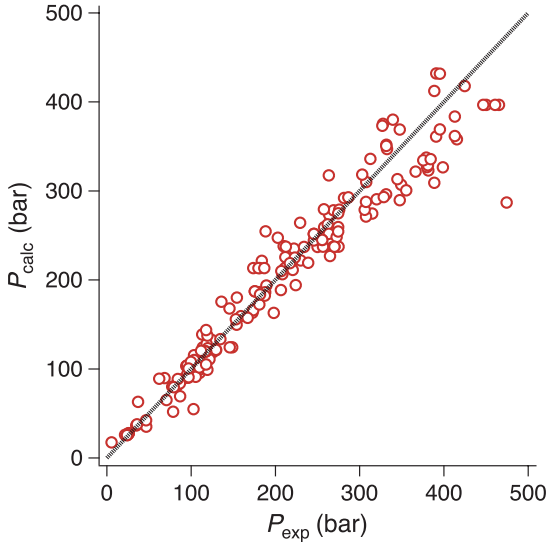

Fig. 6. Comparison of experimental saturation pressures with values calculated by the β model coupled with Eq. 9.

Table 4 Prediction comparison between the beta model (based on Eq. 9) and the correlation of Elsharkawy (2003).

Parameters	Unit	β model	Empirical model (Elsharkawy 2003)
AAD (*P*)	%	10.8	10.3
ARD (*P*)	%	−0.3	−1.4
ARD (x)	%	11.6	–
AAD (x)	%	29.9	–
Mean (σ_x)	mole %	2.7	–

Mean (σ_x), mean relative mean square error between experimental and calculated composition; ARD, average relative deviation; AAD, average absolute deviation.

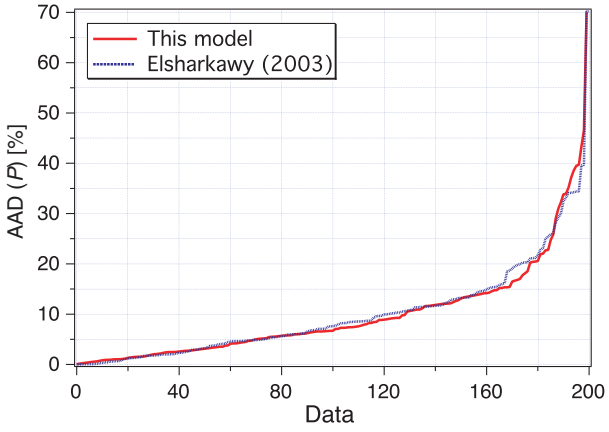

Fig. 7. Average absolute pressure deviation of models with respect to experimental data [full line: the β model of this work; dotted curve: the empirical model of Elsharkawy (2003)].

which has been obtained by multilinear regression on petroleum composition. Figure 7 shows that the β model is as good as this empirical relation, but it is worth noting that the former uses only one independent parameter x_1 instead of the thirteen input variables used in Elsharkawy (2003). Thus, the β model appears to embody much of the physics of crude oils.

Discussion

One question remains, what are the implications of this parameter reduction for the thermodynamic modeling of petroleum inclusions and, in particular, how well is the degree of bubble filling, F_v, calculated by the model? In this model simplification, we assume a 'standard' composition for the nonvolatile part (i.e., an α value fixed at 0.92) for all crude oils: is this standardized model able to reproduce the volumetric properties of unmixed liquid–gas at the temperature T_v as well as the complete α–β model?

A definite answer to this question would require experimental data, but it can be noted that both α–β and β models predict F_v values, which can be quite discrepant (Fig. 8), although they predict consistent saturation pressure and oil composition. Thus, there is some uncertainty about the validity of predicted F_v values, and a better approach would have been to regress α and β values by simultaneous minimizations of the F_3 objective function, defined by:

$$F_3(\alpha,\beta) = (F_{v,calc} - F_{v,exp})^2 \quad (10)$$

with other ones, i.e., F_1 (Eq. 2) and F_2 (Eq. 3). Furthermore, this would have resolved the problem of

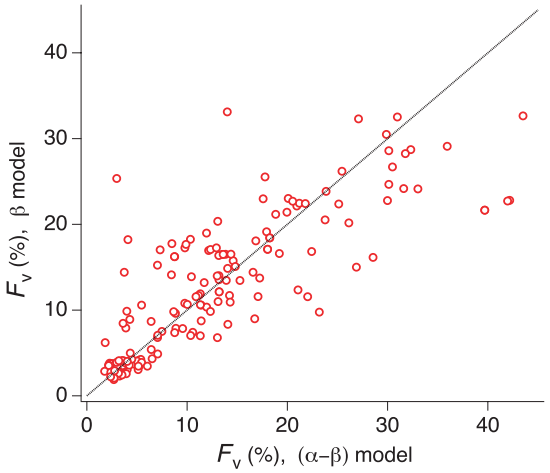

Fig. 8. Comparison of bubble filling degrees F_v calculated by the α–β and β models at 20°C.

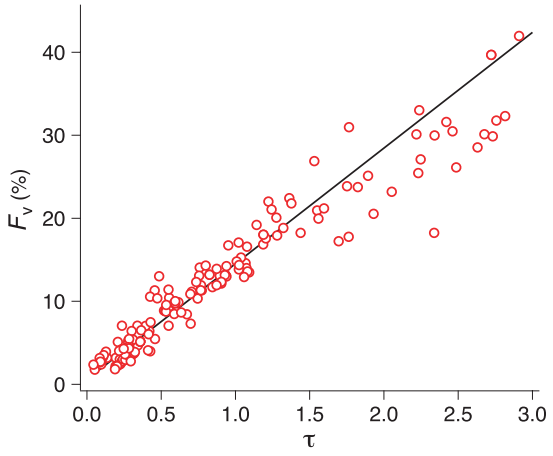

Fig. 9. Linear regression of bubble filling degrees F_v (calculated at 20°C) with the α–β model as a function of the τ parameter.

unconstrained fitting of α and β parameters, as signaled in section Model simplification and to delineate more closely the α–β correlation depicted by petroleum. However, such a work requires many experimental data, including both saturation and flash points measurements, which are still lacking in the literature.

In the previous section, we show that a good representation of saturation pressures can be obtained with a one-parameter model (i.e., the β model) explicit in x_1. Conversely, we have noticed that the degree of bubble filling, F_v, is a complex function of the physico-chemical parameters of the petroleum. Nevertheless, we have found that F_v values (in %) can be correlated linearly as a function of a τ parameter defined by:

$$\tau = \frac{1 - x_{7+}}{x_{7+}}\left(\frac{T_h}{273} - 1\right) \qquad (11)$$

where T_h is expressed in Kelvin. As shown in Fig. 9, the fit is quite good (note also that these are not measured F_v values, but calculated values by the α–β model). A mathematical justification of this relation is given in Appendix, but the important point about this equation is that it is explicit in x_{7+} and not x_1. As a consequence, a complete compositional model for petroleum inclusions should probably involve two independent parameters (as is the case for the α–β model).

Having said that, the β model does not alleviate the major drawback of α–β model, i.e., the nonuniqueness of solutions found for a given petroleum inclusion characterized only by its T_h and F_v values (Thiéry *et al.* 2000, 2002). This was illustrated in Table 1, where the homogenization pressure cannot be assessed with a precision lower than 100 bar (see Table 1 for an illustration of the rather high amplitudes of P_h estimations for inclusions featured by the same T_h and F_v). Regardless, it is recalled that any barometric estimation should involve a critical appraisal of input variables T_h and F_v and their error intervals. The most critical parameter is certainly F_v (Bourdet *et al.* 2008). To illustrate this, we have redone the calculations of Table 1, but with the β model and by taking into account uncertainties on F_v. Adopting typical values found in Bourdet *et al.* (2008), we choose 2% and 4% as the minimal and maximal F_v. Table 5 summarizes the results. This shows that the imprecision on F_v leads here to a strong deterioration of the pressure estimation. Interestingly, the β model provides homogenization pressures P_h with an estimation of the associated errors, which are quite consistent with the α–β model. Thus, from a practical point of view, because of the indeterminations on oil compositions and F_v measurements, the α–β model cannot yield more precise estimations than the β model. Thus, the β model provides a simplified theoretical basis, easier to use, but which should be sufficiently armed to analyze microthermometric and volumetric data of petroleum inclusions.

FLUID MODELS

An alternative to the α–β models is to consider an a priori fluid composition, defined by the mole percents of the different cuts (C_1, C_2, C_3, C_4, C_5, C_6, and C_{7+}) and also by

Table 5 Estimation of the saturation pressure with the β model for a petroleum inclusion featuring a T_h = 54.4°C and a F_v = 3% (±1%) at 20°C.

Solution	F_v (%)	β	P_h (bar)	x_1 (mole %)	x_{7+} (mole %)
1	2	0.054	26	9.3	72.4
2	3	0.0398	89	27.1	48.3
3	4	0.0508	136	37.4	37.3

the characteristics MW_{7+} and SG_{7+} of the C_{7+} fraction. From these data, it is possible, by thermodynamic modeling, to calculate the saturation pressure P_h at the homogenization temperature T_h and the bubble filling degree F_v at temperature T_v. Thus, fluid models require more input data than the α–β model. As a result, these models are more versatile and allow the paraffin/naphthene/aromatic (PNA) nature of the trapped petroleum to be taken into account (if such data are available by gas chromatography (Munz *et al.* 1999; George *et al.* 2007). Paraffinic cuts are characterized by rather high molecular weights (MW) and low densities (SG) (Avaullée *et al.* 2001), whereas aromatic fractions are featured by lower molecular weights and higher densities (naphthene cuts have intermediate values). Calculations, by means of fluid models, are common in petroleum engineering (Ahmed 1989; Pedersen *et al.* 1989).

The method

The basic calculation scheme for fluid models involves several steps detailed below:

(1) splitting of the C_{7+} fraction into a number of pseudocomponents defined by their mole fractions, molecular weights, and specific gravities.
(2) estimation of the physico-chemical properties (critical temperature T_c, critical pressure P_c, critical molar volume V_c, acentric factor ω, and normal boiling temperature T_b) of these pseudocomponents by using appropriate correlations.
(3) lumping of these pseudocomponents into a smaller set of pseudocomponents. The properties of these new pseudocomponents must be assessed from older ones by means of mixing rules.
(4) and finally, use of an equation of state [e.g., Peng & Robinson (1976)] to perform PVT and phase equilibria calculations.

From this general calculation scheme, the number of variants is very large and we have chosen, quite arbitrarily, the following options:

(1) the C_{7+} cut is split into a series of pseudocomponents ranging from C_7 to C_{44}, plus a C_{45+} last term, using the algorithm given in (Ahmed *et al.* 1985). The limiting C_{45+} pseudocomponent was chosen because some correlations [e.g., (Katz & Firoozabadi 1978)] do not define parameters for compounds with higher carbon numbers.
(2) preliminary calculations have shown that calculation results are sensitive to the choice of the correlation used for calculating pseudocomponent parameters (T_c, P_c, T_b, ω). Thus, in this study, we have tested several of them. Several combinations are possible, and this leads us to consider 12 different calculation methods, which are listed in Table 6. Some correlations express the critical properties as a function of boiling temperature T_b and specific gravity SG instead of (MW, SG) laboratory data. In this case, an additional equation is required to link MW, T_b, and SG parameters. Two relations are available in the literature (Whitson 1984; Pedersen *et al.* 1985) and have been tried (Table 6).
(3) pseudocomponents have been lumped into six pseudocomponents, C_7, C_8, C_9, C_{10}, and the last two, called C_{n1} and C_{n2}. C_{n1} groups compounds with carbon atom numbers n between 11 and 25, whereas C_{n2} includes components with n equal or higher than 26. This lumping scheme is the same than the one used in the α–β model (Thiéry *et al.* 2002). Kay's mixing rules (Ahmed 1989; Pedersen *et al.* 1989) have been applied for calculating the parameters (T_c, P_c, ω).
(4) in the testing procedure, we have used only the x_1 and x_{7+} mole fractions given in the data bank. The mole fractions x_2, x_3, x_4, x_5, and x_6 were recalculated

Table 6 List of tested correlations.

Method	T_c, P_c[a]	MW[b]	ω[c]
1	Riazi & Daubert (1987)	–	Edminster (1958)
2	Magoulas & Tassios (1990); Stamataki & Magoulas (2001)	–	Stamataki & Magoulas (2001)
3	Kesler & Lee (1976)	–	Kesler & Lee (1976)
4	Winn (1957)	–	Edminster (1958)
5	Twu (1984)	Pedersen *et al.* (1985)	Edminster (1958)
6	Zhang *et al.* (1998)	Pedersen *et al.* (1985)	Zhang *et al.* (1998)
7	Cavett (1962)	Pedersen *et al.* (1985)	Edminster (1958)
8	Twu (1984)	Whitson (1984)	Edminster (1958)
9	Zhang *et al.* (1998)	Whitson (1984)	Zhang *et al.* (1998)
10	Cavett (1962)	Whitson (1984)	Edminster (1958)
11	Pedersen *et al.* (1988b)	–	Pedersen *et al.* (1988b)
12	Zhang *et al.* (1998)	–	Zhang *et al.* (1998)

(a) references of correlations for calculating the critical temperature, T_c, and the critical pressure, P_c; (b) references for correlations for calculating the molar weight MW from the normal boiling temperature T_b; (c) references of correlations for calculating the acentric factor ω.

by interpolation between x_1 and x_{7+} with the help of Eq. 1 (α and β parameters are calculated from x_1 and x_{7+} values).

(5) PVT calculations are made using the Peng–Robinson equation of state (Peng & Robinson 1976).

(6) binary interaction parameters k_{ij} between hydrocarbons were left to zero.

An important remark should be added with respect to the estimation of molar weights MW_i and specific gravities SG_i of pseudocomponents in the split fluid. In the original version of Ahmed (1989), these parameters are calculated by using the correlations of Katz & Firoozabadi (1978). Then, the parameters for the last-cutting pseudocomponent C_{45+} are calculated from these two equations:

$$\sum_{n=7}^{n=44} x_n \mathrm{MW}_n + x_{45+}\mathrm{MW}_{45+} = x_{7+}\mathrm{MW}_{7+} \tag{12}$$

and

$$\sum_{n=7}^{n=44} \frac{x_n \mathrm{MW}_n}{\mathrm{SG_n}} + \frac{x_{45+}\mathrm{MW}_{45+}}{\mathrm{SG}_{45+}} = \frac{x_{7+}\mathrm{MW}_{7+}}{\mathrm{SG}_{7+}} \tag{13}$$

However, Eqs 12 and 13 were found to yield unrealistic values for MW_{45+} and SG_{45+} (like negative specific gravities) for some sets of MW_{7+} and SG_{7+}. Thus, we preferred to use normalization factors f_M and f_S defined by:

$$f_\mathrm{M} = \frac{x_{7+}\mathrm{MW}_{7+}}{\sum_{n=7}^{n=45} x_n \mathrm{MW}_n^*} \tag{14}$$

$$f_\mathrm{S} = \frac{x_{7+}\mathrm{MW}_{7+}/\mathrm{SG}_{7+}}{\sum_{n=7}^{n=45} x_n \mathrm{MW}_n^*/\mathrm{SG}_n^*} \tag{15}$$

where MW_n^* and SG_n^* are the values calculated by the correlations proposed by (Katz & Firoozabadi 1978). Then, MW_n^* and SG_n^* are calculated by:

$$\begin{aligned} \mathrm{MW}_n &= f_\mathrm{M}\mathrm{MW}_n^* \\ \mathrm{SG}_n &= f_\mathrm{S}\mathrm{SG}_n^* \end{aligned} \tag{16}$$

for n between 7 and 45. Note that MW_{45+} and SG_{45+} are assimilated to MW_{45} and SG_{45} values in these summations.

Correlation comparisons

Table 7 gives the comparison results of the different calculation methods listed in Table 6. The best results are obtained with methods (2), (7), and (11). For the rest of this analysis, we have retained the method (11).

Table 7 Comparison of the different methods for calculating the saturation pressure of crude oils.

Method	ARD (*P*)	AAD (*P*)	Validated
1	−46.4	46.4	
2	1.6	10.9	√
3	−17.7	20.5	
4	−16.5	16.0	
5	−11.7	15.2	
6	−10.2	14.1	
7	5.2	9.6	√
8	−16.2	19.3	
9	−10.1	14.1	
10	−7.3	15.1	
11	−2.7	11.0	√
12	−7.5	12.1	

ARD, average relative deviation; AAD, average absolute deviation.

Model simplification

As for the α–β model, we attempt to build a simplified fluid model that is able to predict the saturation pressures of crude oils, but with a minimal number of input variables. As correlations used in fluid models at least require the characterization of the C_{7+} fraction, we regress experimental x_{7+}, MW_{7+}, and SG_{7+} as a function of x_1. The standard deviation of the residuals between fitted and experimental values is, respectively, of 0.55 for the C_{7+} fraction, 0.03 for SG_{7+}, and 33 g mol^{-1} for MW_{7+}. This yields:

$$\begin{aligned} x_{7+} &= -0.14053 + 0.92164\exp(-1.6511x_1) \\ \mathrm{SG}_7+ &= 0.90411 - 0.13025x_1 \\ \mathrm{MW}_{7+} &= 265.51 - 102.03x_1 \end{aligned} \tag{17}$$

Thus, as for the β model, we can develop a fluid model, which is a function of only one independent variable (x_1). The prediction of this fluid model has been tested, and results are given in Table 8 and Figs 10 and 11. These show that this fluid model can be as predictive as the α–β and the β models. Because it is explicit in x_1, this method appears to be as useful as the β model. Thus, a petroleum inclusion featured by its T_h, F_v, and its hypothesized compositional distribution (C_1, C_2, C_3, C_4, C_5, C_6, C_{7+}) can be fully characterized (P_h and bulk density) by simple tuning of its methane mole fraction x_1. While the simplified fluid model's application is quite attractive, it shares the same limitations as the β model (see Discussion) for the estimation of F_v.

Table 8 Accuracy of the fluid model of this work.

Method	ARD (*P*) (%)	AAD (*P*) (%)
Equations 17	−1.5	8.7

ARD, average relative deviation; AAD, average absolute deviation.

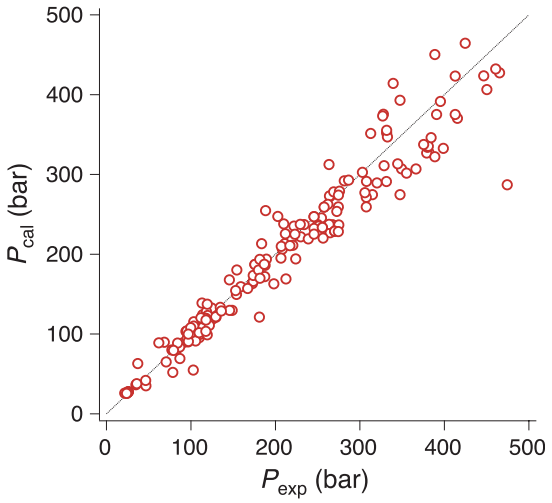

Fig. 10. Comparison of experimental saturation pressures with values calculated by the simplified fluid model of this work.

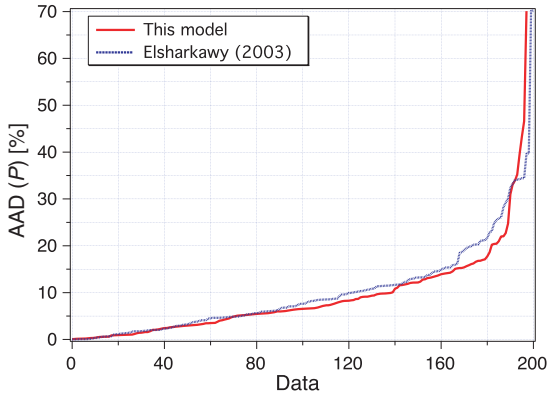

Fig. 11. Average absolute pressure deviation of models with respect to experimental data (full line: the simplified fluid model of this work; dotted curve: the regression equation given in Elsharkawy (2003).

CONCLUSION

Two types of compositional and thermodynamic modeling (α–β and fluid models) have been tested here for their accuracy to predict the saturation pressure of crude oils under typical reservoir *P-T* conditions. From a literature compilation of 201 data points, including measured composition and bubble point pressures, we show that both approaches are able to satisfactorily predict the saturation pressure with <10% AAD of the pressure. For about half of them, the pressure deviation can fall below 5%.

This study also uses evidence of the major control of the bulk methane content onto the homogenization pressure P_h. Thus, it is possible to develop simplified versions of α–β and fluid models, which allow the prediction of the homogenization pressure P_h from T_h and x_1 only. Unfortunately, the volumetric variations of the bubble in the fluid inclusion are not directly linked to x_1, but rather to x_{7+}. For this reason, it is not possible to unambiguously characterize a petroleum inclusion from only its microthermometric signature (T_h, F_v). Nevertheless, we introduce here simplified models, which are easier to use and can provide useful estimates of P_h, x_1, and x_{7+} with their probable error intervals. As a result, this opens the perspective to develop graphical correlations between (T_h, P_h, F_v, x_1, and x_{7+}) for petroleum inclusions, as suggested by Bourdet *et al.* (2008) and which will be easier to use by fluid inclusionists.

The degree of bubble of filling, F_v, (more precisely, the slope of F_v in a F_v–T_h diagram) is a good indicator of the C_{7+} fraction (Fig. 4 in Bourdet *et al.* 2008). Thus, it can reasonably indicate the nature of the petroleum type: heavy black oil, black oil, volatile oil, and gas condensate. This is illustrated by Fig. 9 and Eq. 11. However, the F_v parameter does not carry sufficient information to constrain the *in situ* pressure of the fluids inside the inclusion. In other words, it is a poor barometer, as illustrated by the pressure amplitude in Tables 1 and 5, whichever model is used (alpha–beta or beta models).

The best constraining parameter for pressure modeling is the methane mole fraction. However, this parameter is not easy to measure (i.e., even using FT-IR spectroscopy), and future research efforts should focus on this. Aplin *et al.* (1999) suggested further work on group of fluids that 'are genetically related', in order to alleviate this problem of compositional uncertainty. We agree with this conclusion, as stretching and preferential leakage can be evidenced relatively easily (Bourdet *et al.* 2008). For practical applications, a model such as the beta model could be sufficient. Nevertheless, pressure estimations should be accompanied by an evaluation of the error intervals, which can be large if there is little information on the methane content.

ACKNOWLEDGEMENTS

This work was performed during the visit of H. Ping at the 'Laboratoire Magmas et Volcans (LMV)' of the Blaise Pascal University in France in 2010. Partial support has been provided by the ANR program 'SlabFlux' (K. Koga) about the solubility of volatiles in polymerized fluids. A free calculation program can be downloaded at http://www.obs.univ-bpclermont.fr/lmv/pperm/thiery_r/index.php for thermodynamic modeling of petroleum inclusion. We are grateful to Prof. Aplin A C and an anonymous reviewer for their careful review that helped us to improve an earlier version of this manuscript. We thank also Prof. Richard Worden for his constructive comments.

NOMENCLATURE

T,	Temperature (K)
P,	Pressure (bar)
V,	Molar volume (m^3 mol^{-1})
T_h,	Homogenization temperature (K)
P_h,	Homogenization pressure (bar)
F_v,	Bubble filling degree (%)
T_v,	Measurement temperature of F_v (K)
P_v,	Pressure at T_v (bar)
P_t,	Trapping pressure (bar)
T_t,	Trapping temperature (K)
R,	Gas constant (J mol^{-1} K^{-1})
α,β,	Parameters of the α–β model
n,	Number of carbon atoms
x_i,	Mole fraction of component (or pseudocomponent) i
MW_{7+},	Molar weight of the C_{7+} fraction (g mol^{-1})
SG_{7+},	Specific gravity of the C_{7+} fraction
f_M,f_S,	Renormalization parameters
N_v,	Number of moles in the bubble
N_l,	Number of moles in the liquid
F_1, F_2, F_3,	Objective functions
ARD,	Average relative deviation (%)
AAD,	Average absolute deviation (%)
RMS,	Relative mean square error (%)
Δx,	Absolute deviation between experimental and calculated composition
σ_x,,	Relative mean square error between experimental and calculated composition
exp,	Experimental
calc,	Calculated
N,	Number of data points
T_c,	Critical temperature (K)
P_c,	Critical pressure (bar)
V_c,	Critical molar volume (cm^3 $mol^{-}1$)
ω,	Acentric factor
T_b,	Boiling temperature (K)
k_{ij},	Binary interaction parameter
τ,	Empirical parameter.

REFERENCES

Al-Meshari A (2004) *New Strategic Method to Tune Equation-of-State to Match Experimental Data for Compositional Simulation*. Petroleum Engineering, Texas A&M University, Texas, 248 pp.

Agarwal R, Li Y, Nghiem L (1990) A regression technique with dynamic parameter selection for phase-behavior matching. *SPE reservoir engineering*, **5**, 115–20.

Ahmed T (1989) *Hydrocarbon Phase Behavior*. Gulf Pub. Co., Houston.

Ahmed T, Cady G, Story A (1985) A generalized correlation for characterizing the hydrocarbon heavy fraction. In: *SPE 60th Annual Technical Conference*, Las Vegas, SPE, 14266.

Aplin AC, Macleod G, Larter SR, Pedersen KS, Sorensen H, Booth T (1999) Combined use of Confocal Laser Scanning Microscopyand PVT simulation for estimating the composition andphysical properties of petroleum in fluid inclusions. *Marine and Petroleum Geology*, **16**, 97–110.

Avaullée L, Neau E, Jaubert J-N (1997) Thermodynamic modeling for petroleum fluids II. Prediction of PVT properties of oils and gases by fitting one or two parameters to the saturation pressures of reservoir fluids. *Fluid Phase Equilibria*, **139**, 171–203.

Avaullée L, Duchet-Suchaux P, Durandeau M, Jaubert JN (2001) A new approach in correlating the oil thermodynamic properties. *Journal of Petroleum Science and Engineering*, **30**, 43–65.

Bourdet J, Pironon J, Levresse G, Tritlla J (2008) Petroleum type determination through homogenization temperature and vapour volume fraction measurements in fluid inclusions. *Geofluids*, **8**, 46–59.

Bourdet J, Pironon J, Levresse G, Tritlla J (2010) Petroleum accumulation and leakage in a deeply buried carbonate reservoir, Níspero field (Mexico). *Marine and Petroleum Geology*, **27**, 126–42.

Cavett R (1962) Physical Data for Distillation Calculations–Vapor-Liquid Equilibria. In: Proc. 27th Annual Meeting, American Petroleum Institute, Dallas, 351–66.

Chen H, Wang J, Xie Y, Wang Z (2003) Geothermometry and geobarometry of overpressured environments in Qiongdongnan Basin, South China Sea. *Geofluids*, **3**, 177–87.

Coats K, Smart G (1986) Application of a regression-based EOS PVT program to laboratory data. *SPE reservoir engineering*, **1**, 277–99.

Danesh A, Xu D, Todd A (1992) A grouping method to optimize oil description for compositional simulation of gas-injection processes. *SPE reservoir engineering*, **7**, 343–8.

De Hemptinne J, Béhar E (2006) Thermodynamic Modelling of Petroleum Fluids. *Oil & Gas Science and Technology-Revue de l'IFP*, **61**, 303–17.

Drohm JK, Goldthorpe WH, Trengove R (1988) Enhancing the Evaluation of PVT Data. In: Offshore South East Asia Show Singapore, 1988.

Edminster WC (1958) Applied hydrocarbon thermodynamics Part 4. Compressibility factors and equations of state. *Petroleum Refiner*, **37**, 173–9.

Elsharkawy AM (2003) An empirical model for estimating the saturation pressures of crude oils. *Journal of Petroleum Science and Engineering*, **38**, 57–77.

George SC, Volk H, Ahmed M (2007) Geochemical analysis techniques and geological applications of oil-bearing fluid inclusions, with some Australian case studies. *Journal of Petroleum Science and Engineering*, **57**, 119–38.

Goldstein RH, Reynolds TJ (1994) Systematics of fluid inclusions in diagenetic minerals. In: *SEM Short Course 31*. Society of Sedimentary Geology (SEPM), Tulsa, 199.

González-Partida E, Carrillo-Chávez A, Grimmer JOW, Pironon J, Mutterer J, Levresse G (2003) Fluorite deposits at Encantada–Buenavista, Mexico: products of Mississippi Valley type processes. *Ore Geology Reviews*, **23**, 107–24.

Guillaume D, Teinturier S, Dubessy J, Pironon J (2003) Calibration of methane analysis by Raman spectroscopy in H_2O-NaCl-CH_4 fluid inclusions. *Chemical Geology*, **194**, 41–9.

Hoffman A, Crump J, Hocott C (1953) Equilibrium constants for a gas-condensate system. *Transaction of American Institute of Mining, Metallurgical, and Petroleum Engineers*, **198**, 1–10.

Hong K (1982) Lumped-component characterization of crude oils for compositional simulation. Soc. Pet. Eng. AIME, Pap.

Jacopy RH, Berry VJ (1958) A method for predicting pressure maintenance for reservoirs producing volatile oil. *Petroleum*

Transactions, Transaction of American Institute of Mining, Metallurgical, and Petroleum Engineers, **213**, 59–65.

Jaubert J-N, Neau E, Avaullée L, Zaborowski G (1995) Characterization of Heavy Oils. 3. Prediction of gas injection behavior: swelling test, multicontact test, multiple-contact minimum miscibility pressure, and multiple-contact minimum miscibility enrichment. *Industrial & Engineering Chemistry Research*, **34**, 4016–32.

Jaubert J-N, Avaullée L, Souvay J-F (2002) A crude oil data bank containing more than 5000 PVT and gas injection data. *Journal of Petroleum Science and Engineering*, **34**, 65–107.

Jhaveri B, Youngren G (1988) Three-parameter modification of the Peng–Robinson equation of state to improve volumetric predictions. *SPE reservoir engineering*, **3**, 1033–40.

Katz D, Firoozabadi A (1978) Predicting phase behavior of condensate/crude-oil systems using methane interaction coefficients. *Journal of Petroleum Technology*, **30**, 1649–55.

Kesler M, Lee B (1976) Improved prediction of enthalpy of fractions. *Hydrocarbon Processing*, **55**, 153–8.

Kissin YV (1987) Catagenesis and composition of petroleum: origin of n-alkanes and isoalkanes in petroleum crudes. *Geochimica et Cosmochimica Acta*, **51**, 2445–57.

Li Y, Nghiem L, Siu A (1985) Phase behavior computations for reservoir fluids: effect of pseudo-components on phase diagrams and simulation results. *Journal of Canadian Petroleum Technology*, **24**, 29–36.

Macleod G, Larter SR, Aplin AC, Pedersen KS, Booth TA (1996) Determination of the effective composition of single petroleum inclusions using confocal scanning laser microscopy and PVT simulation. In: *Biennial Pan-American Conference on Research on Fluid Inclusions (PACROFI VI)* (eds Brown PE, Hagemann SG), pp. 81–82. Elsevier, Madison, WI.

Magoulas K, Tassios D (1990) Thermophysical properties of n-alkanes from C_1 to C_{20} and their prediction for higher ones. *Fluid Phase Equilibria*, **56**, 119–40.

McCain Jr. WD (1990) *The Properties of Petroleum Fluids*. 2nd edn. Pennwell Publishing Company,Tulsa, 548 pp.

McCain Jr. WD (1994) Heavy components control reservoir fluid behavior. *Journal of Petroleum Technology*, **46**, 746–50.

Moharam HM (1995) Prediction of viscosity of heavy petroleum fractions and crude oil using a corresponding states method. *Industrial & Engineering Chemistry Research*, **34**, 4140–4.

Montel F (1993) Phase equilibria needs for petroleum exploration and production industry. *Fluid Phase Equilibria*, **84**, 343–67.

Munz IA (2001) Petroleum inclusions in sedimentary basins: systematics, analytical methods and applications. *Lithos*, **55**, 195–212.

Munz IA, Johansen H, Johanse I (1999) Characterisation of composition and PVT properties of petroleum inclusions: implications of reservoir filling and compartmentalisation. *Society of Petroleum Engineers*, **56519**, 1–7.

Neau E, Jaubert JN, Rogalski M (1993) Characterization of heavy oils. *Industrial & Engineering Chemistry Research*, **32**, 1196–203.

Pedersen KS, Rasmussen P, Fredenslund A (1985) Thermodynamics of petroleum mixtures containing heavy hydrocarbons. 3. Efficient flash calculation procedures using the SRK equation of state. *Industrial & Engineering Chemistry Process Design and Development*, **24**, 948–54.

Pedersen KS, Thomassen P, Fredenslund A (1988a) On the danger of tuning equation of state parameters. *Chemical Engineering Science*, **43**, 269–78.

Pedersen KS, Thomassen P, Fredenslund A (1988b) Characterization of gas condensate mixtures. In: AIChE Spring National Meeting, New Orleans, Louisiana.

Pedersen K, Fredenslund A, Thomassen P (1989) *Properties of Oils and Natural Gases*. Gulf Pub. Co., Houston.

Peng D, Robinson D (1976) A new two-constant equation of state. *Industrial & Engineering Chemistry Fundamentals*, **15**, 59–64.

Pironon J (2004) Fluid inclusions in petroleum environments: analytical procedure for PTX reconstruction. *Acta Petrologica Sinica*, **20**, 1333–42.

Pironon J, Canals M, Dubessy J, Walgenwitz F, Laplace-Builhe C (1998) Volumetric reconstruction of individual oil inclusions by confocal scanning laser microscopy. *European Journal of Mineralogy*, **10**, 1143–50.

Pironon J, Thiery R, Ayt Ougougdal M, Teinturier S, Beaudoin G, Walgenwitz F (2001) FT-IR measurements of petroleum fluid inclusions: methane, n-alkanes and carbon dioxide quantitative analysis. *Geofluids*, **1**, 2–10.

Riazi MR, Daubert TE (1987) Characterization parameters for petroleum fractions. *Industrial & Engineering Chemistry Research*, **26**, 755–9.

Riemens W, Schulte A, de Jong LNJ (1988) Birba field PVT variations along the hydrocarbon column and confirmatory field tests. *Journal of Petroleum Technology*, **40**, 83–8.

Roedder E (1984) *Fluid Inclusions*. Mineralogical Society of Canada, Washington.

Rosenegger L, Wu R (1999) Intergrated oil PVT data characterization-lessons from four case histories. *Journal of Canadian Petroleum Technology*, ***Spec. Ed. 38**, (Paper 97-05)*.

Stamataki SK, Magoulas KG (2001) Characterization of Heavy Undefined Fractions. In: SPE International Symposium on Oilfield Chemistry, Houston, Texas, SPE, 64996.

Teinturier S, Pironon J, Walgenwitz F (2002) Fluid inclusions and PVTX modelling: examples from the Garn Formation in well 6507/2-2, Haltenbanken, Mid-Norway. *Marine and Petroleum Geology*, **19**, 755–65.

Thiéry R, Pironon J, Walgenwitz F, Montel F (2000) PIT (Petroleum Inclusion Thermodynamic): a new modeling tool for the characterization of hydrocarbon fluid inclusions from volumetric and microthermometric measurements. *Journal of Geochemical Exploration*, **69–70**, 701–4.

Thiéry R, Pironon J, Walgenwitz F, Montel F (2002) Individual characterization of petroleum fluid inclusions (composition and P-T trapping conditions) by microthermometry and confocal laser scanning microscopy: inferences from applied thermodynamics of oils. *Marine and Petroleum Geology*, **19**, 847–59.

Twu CH (1984) An internally consistent correlation for predicting the critical properties and molecular weights of petroleum and coal-tar liquids. *Fluid Phase Equilibria*, **16**, 137–50.

Vogel JL, Yarborough L (1980) The effect of nitrogen on the phase behavior and physical properties of reservoir. In: *SPE/DOE Enhanced Oil Recovery Symposium*. Society of Petroleum Engineers, Tulsa, OK.

VTFlinc (1997) User's guide. In: *Lingby*, CALSEP A/S, Chemical Engineering Consulting, Lyngby, Denmark.

Wang LS, Gmehling J (1999) Improvement of SRK equation of state for vapor-liquid equilibria of petroleum fluids. *AiChE Journal*, **45**, 1125–34.

Whitson C (1984) Effect of C_{7+} properties on equation-of-state predictions. *Society of Petroleum Engineers Journal*, **24**, 685–96.

Williams C, Zana E, Humphrys G (1980) Use of the Peng–Robinson equation of state to predict hydrocarbon phase behavior

and miscibility for fluid displacement. In: *SPE/DOE Enhanced Oil Recovery Symposium*. Tulsa, Oklahoma, SPE, 8817.
Winn F (1957) Physical Properties by Nomogram. *Petroleum Refiner*, **36**, 157–9.
Yang T, Chen WD, Guo TM (1997) Phase behavior of a near-critical reservoir fluid mixture. *Fluid Phase Equilibria*, **128**, 183–97.
Zhang J, Zhao S, Wang R, Yang G (1998) Prediction of critical properties of non-polar compounds, petroleum and coal-tar liquids. *Fluid Phase Equilibria*, **149**, 103–9.

APPENDIX

An empirical relationship between F_v and x_{7+}

Section Discussion presents a linear correlation between bubble filling degree F_v and a parameter τ (Eq. 11). This empirical relation can be justified as follows. First, we start from the definition of the bubble filling degree F_v

$$F_v = \frac{N_g V_g}{N_g V_g + N_l V_l} \tag{18}$$

where N_g and N_l are the number of moles in the gas and liquid and V_g and V_l are the respective molar volumes. For petroleum inclusions homogenizing to liquid, F_v is below 50%, and crude oils have typically F_v below 20% (Bourdet *et al.* 2008). Thus, we assume $N_g V_g$ is negligible against $N_l V_l$:

$$F_v \approx \frac{N_g V_g}{N_l V_l} \tag{19}$$

the major component in the bubble is methane. However, the amount of exsolved methane is limited by its solution in the liquid, which acts as a 'sponge'. Thus, we assume that N_g is given by:

$$N_g \propto x_1 \times (1 - x_{7+}) \tag{20}$$

the liquid is predominantly composed of the C_{7+} fractions. Thus,

$$N_l \propto x_{7+} \tag{21}$$

the gas can be considered as a perfect gas. Therefore,

$$V_g = \frac{RT_v}{P_v} \propto \frac{1}{P_v} \tag{22}$$

moreover, the *in situ* pressure P_v at temperature T_v is well correlated with the homogenization pressure P_h: the higher the P_h, the greater the P_v. To a first approximation, we can assume:

$$P_v \propto P_h \tag{23}$$

from Fig. 3, we can approximate P_h as a linear function of x_1:

$$P_h \propto x_1 \tag{24}$$

thus, from Eqs 22–24, we get:

$$V_g \propto \frac{1}{x_1} \tag{25}$$

and finally, the liquid molar volume V_l is given by:

$$V_l = \frac{MW_{7+}}{SG_{7+}} \tag{26}$$

but will be treated as a constant.

Integration of these assumptions into Eq. 18 yields:

$$F_v \propto \frac{x_1 \times (1 - x_{7+})}{x_1} \frac{1}{x_{7+}} \tag{27}$$

Thus, after elimination of x_1, one obtains:

$$F_v \propto \frac{1 - x_{7+}}{x_{7+}} \tag{28}$$

This latter equation is valid for inclusions homogenizing at the same T_h. To take into account the influence of different T_h (the higher the T_h, the greater is F_v), we add an additional factor as follows:

$$F_v \propto \frac{1 - x_{7+}}{x_{7+}} \left(\frac{T_h}{273} - 1 \right) \tag{29}$$